

Ionization-free resonantly enhanced low-order harmonic generation in a dense gas mixture by a mid-IR laser field

E. A. Migal ^{1,2}, S. Yu. Stremoukhov ^{1,3} and F. V. Potemkin ^{1,2,*}

¹*Faculty of Physics, M.V. Lomonosov Moscow State University, Leninskie Gory bld.1/2, 119991 Moscow, Russia*

²*International Laser Center, M.V. Lomonosov Moscow State University, Leninskie Gory bld.1/62, 119991 Moscow, Russia*

³*National Research Centre “Kurchatov Institute,” pl. Akademika Kurchatova, 1, Moscow 123182, Russia*



(Received 2 November 2019; accepted 9 January 2020; published 5 February 2020)

Recent advances in the development of powerful transition-metal-doped chalcogenide femtosecond lasers made it possible to produce laser radiation directly in the vicinity of molecular vibrational resonances. Here we demonstrate the use of such light for low-order harmonic generation in a dense gas mixture, containing carbon dioxide molecules resonantly interacting with pump radiation. We report on the manifold increase of third (25) and fifth (10) harmonic generation efficiency and the appearance of subsequent harmonics (from 7th to 11th) in xenon (48 bars) in the presence of carbon dioxide (1 bar). Final conversion efficiency obtained experimentally and confirmed numerically reaches 1% for third harmonic and 0.3% for higher ones (from 5th to 11th in total) under a very moderate vacuum intensity of 1.8×10^{13} W/cm². These experiments open new perspectives for optimization of harmonic generation efficiency without significant perturbation of the media. In particular, phase-matching conditions may be also found in extreme ultraviolet and soft x-ray regions, where conversion efficiency from a mid-IR pump stays quite low.

DOI: [10.1103/PhysRevA.101.021401](https://doi.org/10.1103/PhysRevA.101.021401)

I. INTRODUCTION

The interaction of laser radiation with resonant media is one of the classic problems at the junction of nonlinear optics and laser physics. It has been extensively studied since the appearance of laser sources and was directed on the understanding of numerous observed resonant phenomena such as self-induced transparency [1], self-focusing [2], and efficient wave mixing [3], and on shedding light upon extreme regimes in nonlinear optics in quest of limits to supreme nonlinear conversion in laser-matter interaction processes [4]. Experimental and theoretical approaches that had been developed in these works revealed important aspects of the interaction of laser radiation with two-level systems and resulted in the production of slow light [5], the development of devices based on saturated absorption [6]. Recently problems of resonant light-matter interactions have been addressed anew in the view of low- and high-harmonic generation processes since in this case atomic resonances may induce enhancement of the harmonics yield [7,8], lead to strong polarization-state variations [9], and potentially reveal the dynamics of bound and quasibound states in the presence of a strong driving field [10]. Several mechanisms for resonant enhancement have been discussed in the literature, involving an intermediate resonant step in the semiclassical three-step model. Additional resonant steps may occur either in the ionization process, via a multiphoton resonance between the ground state and the Stark-shifted excited state, or in the rescattering process via electron trapping into an autoionizing state that enhances the probability of the process [10–12]. Notably, such approaches

provide enhancement of single or just a few harmonics in the spectrum.

The development of high power mid-IR sources [13–18] provides direct access to molecular resonances lying in the range between 2 and 10 μm that is actively exploited for spectroscopy and remote sensing. Creation of such sources is also stimulated by scaling of the mean quiver energy of the electron in the laser field as a product of laser intensity and squared wavelength $\sim I \times \lambda^2$ giving the opportunity to reach water window, the region hardly achievable with the ubiquitous Ti:sapphire driver. However, the transition to shorter x-ray wavelengths comes at a cost in terms of photon flux, which scales as $\lambda^{-5.5}$ [19]. Therefore, phase matching of a large number of emitters and enhancement of harmonics yield is of particular importance for further applications of such sources.

In this Rapid Communication, we propose the idea of the usage of molecular resonances located near the pump spectrum for enhancement of harmonics yield driven by mid-IR fields. We exploit favorable wavelengths of our mid-IR driver in order to achieve a manifold increase of conversion efficiency to the first 11 harmonics in the presence of resonant molecules. Our concept is verified both experimentally and numerically at low-order harmonics and shown to be useful for high orders through theoretical considerations.

II. EXPERIMENTAL SETUP

A mid-IR chirped pulse amplification (CPA) system based on Fe:ZnSe crystal was used to generate harmonics in a gas mixture (Fig. 1). A detailed description of the system can be found elsewhere [18]. Briefly, a Fe:ZnSe amplifier was optically pumped by 2.85- μm , 90-mJ laser pulses produced by a Cr:Yb:Ho:YSGG laser. As a seed source, a mid-IR

*potemkin@physics.msu.ru

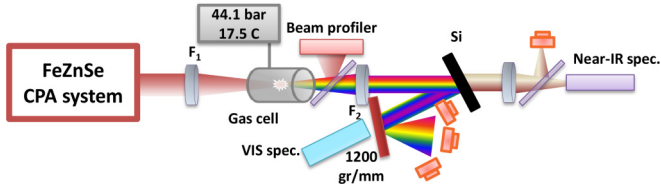


FIG. 1. Experimental setup: F_1 and F_2 are focusing and collimating lenses; Si is silicon plate.

optical parametric amplifier was used. An amplification band of the Fe:ZnSe system partially overlaps with the absorption spectrum of atmospheric CO_2 ; therefore, the whole system operates in a vacuum chamber to prevent any spectral distortions. CPA generates 150-fs pulses with up to 3.5 mJ energy centered at 4.4 μm . Part of the output energy was focused to a beam diameter of 160 μm ($1/e$) by a 150-mm uncoated CaF_2 lens, resulting in a vacuum peak intensity of 1.8×10^{13} W/cm^2 . We used an 8-cm gas cell equipped with 6-mm-long uncoated CaF_2 windows. To deliver the shortest pulse duration and compensate group velocity dispersion from the windows and focusing lens we adjusted the distance between the grating pair in the CPA compressor. The pressure and temperature inside the cell was controlled with an accuracy of 0.1 bar and 0.1 C. The output beam was collimated by an uncoated 50-mm CaF_2 lens and analyzed by the following equipment. For spectral measurements in the UV and visible range (300–1100 nm) the short-wavelength part of the harmonics radiation was reflected off by a 0.1-mm Si plate to be detected by a Solar USB TII spectrometer. The transmitted part of the radiation was directed to a SDH IV near-IR spectrometer for measurements in the 0.9–2.5 μm spectral range. The mid-IR part of the spectrum was characterized using a scanning monochromator and a PbSe detector. The beam profile of the pump radiation was measured by a Spiricon Pyrocam III. For energy measurements the pump beam was blocked by a 20-mm-thick quartz plate. The visible part of the harmonics (fifth to ninth harmonics) was spectrally selected by 1200 g/mm diffraction grating and a set of bandpass color filters. The third harmonic signal was measured after Si plate. In the experiments high-purity xenon and carbon dioxide gases were used.

III. RESULTS

Firstly, we examined the generation of low-order harmonics in pure xenon. In this case the generation of third and fifth harmonics with maximum efficiency of 0.05% and 0.01% was observed at around 44 bars. Note that the input pulse peak power of 3.7 GW corresponds to 0.5–1 P_{cr} in xenon, where P_{cr} is a critical power for self-focusing. Visually we did not observe any plasma channel inside the cell, while the total electron concentration estimated from the Ammosov-Delone-Krainov (ADK) ionization model stayed below 10^{15} cm^{-3} . Pump losses were confirmed to be below 3%, attributed to instability of the driving source. Therefore, the harmonics are generated without onset of the filamentation. The observed conversion efficiency is of the same order of magnitude as was reported previously under filamentation in noble gases [20] and air [13,21]. In general, due to the sufficiently lower

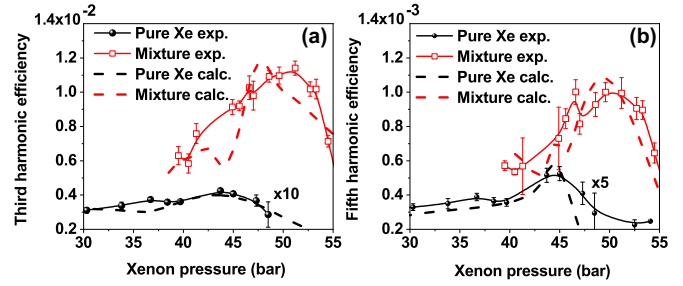


FIG. 2. Third (a) and fifth (b) harmonic efficiency as a function of xenon pressure in the case of pure gas (black circles) and a mixture of gases (red open squares). Solid and dashed lines represent experimental and calculated data.

dispersion of gases in the mid-IR spectral region low-order harmonics driven by mid-IR fields are generated more efficiently compared to the near-IR pump (such as 800 nm). In our measurements, harmonics efficiency increases with pressure until reaching a maximum at around 44 bars followed by the decrease in its yield (Fig. 2). Two main factors define non-monotonic dependence of harmonics conversion efficiency. With an increase of pressure phase mismatch between harmonics becomes stronger, while gas nonlinearity sufficiently grows. To further increase conversion efficiency it is natural to find media with higher nonlinearity or to use specialized phase-matching techniques. Recently, it was proposed that a nonlinear refractive index of carbon dioxide near 4.3 μm resonance band can reach 10^{-12} cm^2/W for 100 Torr [22]. Since the spectrum of our laser source also partially overlaps with this absorption band, the influence of carbon dioxide molecules in a gas mixture has been studied.

To check this idea we fixed the xenon pressure at around 44–45 bars and prepared different mixtures of xenon with small amounts of CO_2 (0.1–2.5 bars). At a partial pressure of 1–1.3 bars we have observed the generation of odd optical harmonics up to 11th order, for which the spectra are presented in Fig. 3. Figure 4 demonstrates the evolution of third to ninth harmonics yield with CO_2 partial pressure. Approaching a pressure of 1 bar, third and fifth harmonic efficiency increases 25 and 10 times reaching 1.2% and 0.1%, respectively. The total efficiency to the harmonics from 5th to 11th was more than 0.3%. Note that conversion efficiency was calculated relative to the input pump energy. However, since

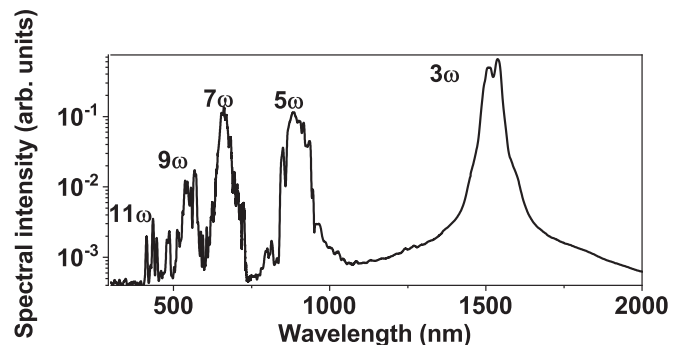


FIG. 3. Harmonics emission from a gas mixture containing 44 bars of xenon and 1 bar of carbon dioxide.

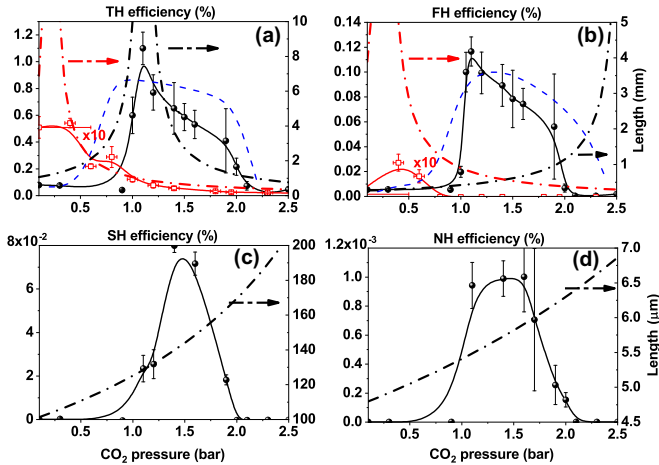


FIG. 4. Evolution of the yield (solid lines) and coherence length (dash-dotted lines) with CO_2 pressure for third (a), fifth (b), seventh (c), and ninth (d) harmonic in gas mixture (black circles) and pure CO_2 (red open squares). Blue dashed lines shows calculated data.

the pump spectrum stays in the vicinity of the absorption line, it is significantly absorbed during propagation. Around 1 bar partial pressure less than 45% of energy is transmitted through the cell. We also did not observe any changes in pump beam profile attributed to self-focusing or self-defocusing.

IV. DISCUSSION

Since the pump beam profile stays unchanged, carbon dioxide only slightly changes gas nonlinearity. This is also confirmed by an order of magnitude decrease of the third and fifth harmonic yield in pure CO_2 gas [Figs. 4(b) and 4(c), red dashed curves] and an absence of higher harmonics. However, in pure gas optimal pressure is shifted, which indicates a significant contribution of CO_2 to phase matching. To explain harmonic yield pressure dependence we calculated coherence length as a function of CO_2 partial pressure. Coherence length includes medium, free-electron, and geometric contributions in full analogy with [23]. The refractive index and transmission of the pump pulse near the absorption band of carbon dioxide is calculated using available HITRAN data [24]. Gas ionization is taken into account through the ADK theory as mentioned above. Note that the absorption length at a particular wavelength of $4.4 \mu\text{m}$ is around 2.8 mm at 1 bar pressure. However, since the absorption spectrum of CO_2 consists of multiple rovibrational transitions the total transmission of the broadband radiation is much higher. As shown in Figs. 4(b) and 4(c) the CO_2 pressure fully controls the coherence length for a particular harmonic and provides phase matching even in pure gas. However, strong absorption and temporal distortion of the driving pulse requires quite high nonlinearity, which is achieved by additional mixing with xenon. The calculations provided above have been made for the central wavelength of the pulse ($4.4 \mu\text{m}$). An instantaneous change of the refractive index near the resonance allows for exact matching of the refractive indices of the pump and harmonics spectral components. Higher harmonic orders lie closer to xenon first electron resonance and, therefore, propagate with higher refractive index. In order to compensate for this change, the pump spectral

components should also have a higher refractive index, which could be obtained even close to carbon dioxide resonance. Therefore, the coherence length for a particular harmonic may be even longer than calculated assuming a $4.4 \mu\text{m}$ driving wavelength. Phase matching of higher harmonics is restricted by strong absorption of the pump in this region leading to the limited number of harmonics observed in the experiment.

To further prove the phase-matching conditions discussed above we have used the one-dimensional interference model which can take into account single-atom responses calculated quantum mechanically exactly with the laser field parameters changing along with its propagation in the gas cell [25]. This approach is simpler than some of those presented previously [26,27] and, at the same time, contrary to that mentioned above, gives the possibility to take into account more consistently the influence of the pressure on the harmonics generation, since the model does not impose any restrictions on this value. The interference model was previously verified by the experiment as well [28]. The model describes third and fifth harmonics efficiency dependencies generated in both pure xenon and a mixture of gases. The pure xenon gas was simulated as continuous matter, while the mixture of gases was simulated as perforated by CO_2 molecules xenon gas for full account of the quasi-phase-matching phenomenon [28]. The corresponding dependencies nicely match the measured ones [see Figs. 2 (black and red dashed lines) and 4 (blue dashed lines)]. The nonlinear dependencies presented in the above-mentioned figures can be explained in terms of constructive and destructive interference of the harmonics generated by single atoms occupying different positions on the path of the laser field. Third and fifth harmonics efficiency grows along with the gas pressure due to the increase of the numbers of harmonics' emitters while all of them interact with the laser field having similar parameters (the shape of the laser field is not drastically changed). Then the parameters of the laser field changed more significantly inside the gas cell; as a result, the first and the last atom emit harmonics which interfere destructively. As a result, the efficiency of the harmonics yield decreases along with the increase of the gas pressure while more and more atoms generate radiation which interfere destructively. Adding the CO_2 gas breaks the harmonics phase distortions and paves the way to further growth of positively interfering harmonics' emitters with the gas pressure. As a result the optimal pressure for the mixture of gases shifts towards the higher xenon pressures.

An instantaneous change of the refractive index in the vicinity of the pump spectrum in addition to the quite low CO_2 ionization potential of 13.8 eV allows for phase matching with almost arbitrary wavelength by adjusting the gas pressure. In this case CO_2 provides a quite large phase mismatch, which cancels the contribution of plasma and the Gouy phase introduced by external focusing. In this approach high gas pressures and complex phase-matching schemes can be eliminated. Figure 5 demonstrates the dependence of the coherence length for harmonics from 101st to 1001st order in a CO_2 gas. Calculations have been done for the same focusing geometry and pump wavelength. Vacuum intensity was taken as $5 \times 10^{13} \text{ W/cm}^2$, resulting in an electron ponderomotive energy of 90 eV, which corresponds to a cutoff energy of 300 eV (1001th harmonic). As can be seen from Fig. 5, the coherence

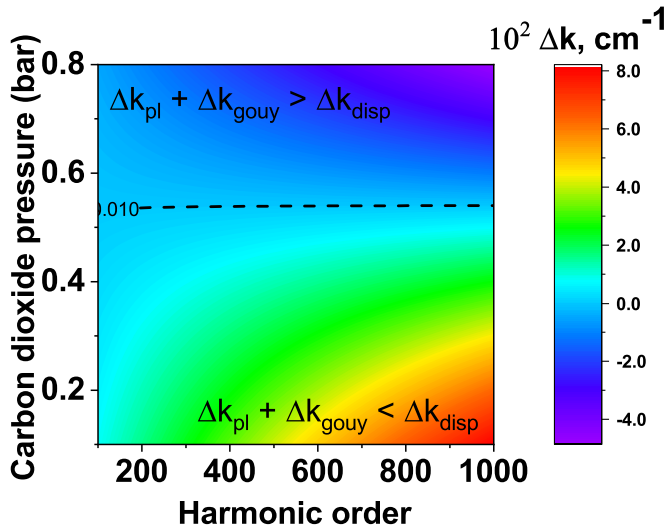


FIG. 5. Phase mismatch in the extreme ultraviolet (EUV) region for different CO₂ pressures and harmonic orders.

length may reach several millimeters, while fine adjusting of the CO₂ pressure allows for broadband phase matching. High harmonics can be perfectly phase matched by balancing the neutral atom dispersion with the dispersion of free-electron plasma including geometric contribution. To avoid significant

absorption of the pump radiation (to maintain the highest intensity) a few-millimeter tube instead of a gas cell can be used in the experiment.

V. CONCLUSIONS

In conclusion, we have proposed a concept for harmonics efficient phase matching using molecular resonances. As a proof-of-principle we generate 11 harmonics in a dense gas mixture containing carbon dioxide, the absorption spectrum of which partially overlaps with the pump radiation. Conversion efficiency as high as 1% for third harmonic and 0.3% for harmonics from 5th to 11th in total is reached. We believe that this concept would be useful for enhancing conversion efficiency into EUV and soft x-ray regions with mid-IR laser drivers.

ACKNOWLEDGMENTS

This work was supported by Russian Foundation for Basic Research (RFBR) (Projects No. 17-02-01065, No. 18-29-20074, and No. 19-29-12030) and partly by the M. V. Lomonosov Moscow State University Program of Development. E.A.M. thanks the Foundation for the Advancement of Theoretical Physics “BASIS.”

- [1] S. L. McCall and E. L. Hahn, *Phys. Rev. Lett.* **18**, 908 (1967).
- [2] D. Grischkowsky, *Phys. Rev. Lett.* **24**, 866 (1970).
- [3] M. S. Dzhdzhoev, V. T. Platonenko, and A. V. Chugunov, *Sov. J. Quantum Electron.* **15**, 1451 (1985).
- [4] S. Akhmanov, in *Nonlinear Spectroscopy*, edited by N. Bloembergen (North-Holland, Amsterdam, 1979), p. 239.
- [5] L. Vestergaard Hau, S. E. Harris, Z. Dutton, and C. H. Behroozi, *Nature (London)* **397**, 594 (1999).
- [6] B. K. Garside and T. K. Lim, *J. Appl. Phys.* **44**, 2335 (1973).
- [7] P. Ackermann, H. Münch, and T. Halfmann, *Opt. Express* **20**, 13824 (2012).
- [8] R. A. Ganeev, P. A. Naik, H. Singhal, J. A. Chakera, and P. D. Gupta, *Opt. Lett.* **32**, 65 (2007).
- [9] A. Ferré, C. Handschin, M. Dumergue, F. Burgy, A. Comby, D. Descamps, B. Fabre, G. A. Garcia, R. Géneaux, L. Merceron, E. Mével, L. Nahon, S. Petit, B. Pons, D. Staedter, S. Weber, T. Ruchon, V. Blanchet, and Y. Mairesse, *Nat. Photonics* **9**, 93 (2015).
- [10] V. Strelkov, *Phys. Rev. Lett.* **104**, 123901 (2010).
- [11] R. Taieb, V. Vénier, J. Wassaf, and A. Maquet, *Phys. Rev. A* **68**, 033403 (2003).
- [12] P. V. Redkin, M. K. Kodirov, and R. A. Ganeev, *J. Opt. Soc. Am. B* **28**, 165 (2011).
- [13] H. Liang, D. L. Weerawarne, P. Krogen, R. I. Grynko, C.-J. Lai, B. Shim, F. X. Kärtner, and K.-H. Hong, *Optica* **3**, 678 (2016).
- [14] L. von Grafenstein, M. Bock, D. Ueberschaer, K. Zawilski, P. Schunemann, U. Griebner, and T. Elsaesser, *Opt. Lett.* **42**, 3796 (2017).
- [15] X. Ren, L. H. Mach, Y. Yin, Y. Wang, and Z. Chang, *Opt. Lett.* **43**, 3381 (2018).
- [16] Y. Fu, B. Xue, K. Midorikawa, and E. J. Takahashi, *Appl. Phys. Lett.* **112**, 241105 (2018).
- [17] P. Wang, Y. Li, W. Li, H. Su, B. Shao, S. Li, C. Wang, D. Wang, R. Zhao, Y. Peng, Y. Leng, R. Li, and Z. Xu, *Opt. Lett.* **43**, 2197 (2018).
- [18] E. Migal, A. Pushkin, B. Bravy, V. Gordienko, N. Minaev, A. Sirotkin, and F. Potemkin, *Opt. Lett.* **44**, 2550 (2019).
- [19] J. Tate, T. Augustine, H. G. Muller, P. Salières, P. Agostini, and L. F. DiMauro, *Phys. Rev. Lett.* **98**, 013901 (2007).
- [20] D. Kartashov, S. Ališauskas, A. Pugžlys, A. Voronin, A. Zheltikov, M. Petrarca, P. BÉjot, J. Kasparian, J.-P. Wolf, and A. Baltuška, *Opt. Lett.* **37**, 3456 (2012).
- [21] P. Panagiotopoulos, P. Whalen, M. Kolesik, and J. V. Moloney, *Nat. Photon.* **9**, 543 (2015).
- [22] J. J. Pigeon, D. Tovey, S. Y. Tochitsky, G. J. Louwrens, I. Ben-Zvi, D. Martyshev, V. Fedorov, K. Karki, S. Mirov, and C. Joshi, *Phys. Rev. A* **100**, 011803(R) (2019).
- [23] T. Popmintchev, M. C. Chen, A. Bahabad, M. Gerrity, P. Sidorenko, O. Cohen, I. P. Christov, M. M. Murnane, and H. C. Kapteyn, *Proc. Natl. Acad. Sci. USA* **106**, 10516 (2009).
- [24] R. V. Kochanov, I. E. Gordon, L. S. Rothman, P. Wcisło, C. Hill, and J. S. Wilzewski, *J. Quant. Spectrosc. Radiat. Transfer* **177**, 15 (2016).
- [25] S. Y. Stremoukhov and A. V. Andreev, *Laser Phys.* **28**, 035403 (2018).
- [26] M. B. Gaarde, J. L. Tate, and K. J. Schafer, *J. Phys. B* **41**, 132001 (2008).
- [27] E. Lorin, S. Chelkowski, and A. Bandrauk, *Comput. Phys. Commun.* **177**, 908 (2007).
- [28] R. A. Ganeev, S. Y. Stremoukhov, A. V. Andreev, and A. S. Alnaser, *Appl. Sci.* **9**, 1701 (2019).